Environmental Earth Sciences (2021) 80:397
https://doi.org/10.1007/s12665-021-09481-1

ORIGINAL ARTICLE

An introduction to the modeling of active fault zone width's effect on the qualitative deformation of lifelines and their routing (case study: buried gas pipelines in east of Iran)

Babak Kheradmand[1] · Behnam Rahimi[1] · Nasser Hafezi Moghaddas[1] · Majid Mehrizi[2]

Received: 11 May 2020 / Accepted: 4 February 2021 / Published online: 23 May 2021

Abstract
Among the many factors causing damage to lifelines, there are active faults along the pipeline route that can cause fracture and breakdown of the pipeline if it is justified. Thus, during pipeline route study phase, detailed geological work on the route should be undertaken and fault paths identified. It is, therefore, essential to study the structures of the study area to select the appropriate path. Due to crossing of Iranshahr–Mirjaveh gas pipeline in the eastern part of Iran at the intersection with the southern terminals of the Nosrat-Abad fault system, careful study of the geology and structural interpretation of these faults in terms of damage to the pipeline is necessary. Therefore, in this study, fault displacements and damages considering fault width at intersection with lifelines (buried gas pipelines) are modeled and evaluated by special software programs. Therefore, in this paper, considering a specific area in eastern Iran and using available software to simulate the active fault and analyze their effects on pipelines and considering the impact of active fault zones on three issues selected (strike-slip, strike-slip–reverse and reverse faults) have been investigated to improve the design parameters routing of lifelines (buried gas pipelines) in the future.

Keywords Active fault · Lifelines · Modeling · Routing

Introduction

During earthquakes, persistent deformations of the earth can be caused by faults, liquefaction, and so on. Buried pipes can be damaged under displacement or earthquake waves. For example, surface faults in the 1971 San Fernando earthquake broke and buckled gas pipes in the San Fernando fault zone. Similarly, in 1972, the Managua earthquake caused surface displacement in four dominant strike-slip faults in the downtown area and nearly all major water pipes passing through the fault had fractured (ALA 2001).

The Iran range is one of the world's most earthquake-prone areas in the middle of the Alpine–Himalayan orogenic belt. This belt extends from the western Pacific to the eastern Atlantic and is the global intra-continental seismic belt. In the meantime, Iran, as part of this seismic zone, has repeatedly been the site of devastating earthquakes and heavy casualties, so that in the past century alone, more than 100,000 people have been killed. The victims of this natural disaster have become homeless (Zare and Kamranzad 2014).

In the meantime, given the seismicity of the Iranian plateau and having about 40,000 km of gas pipelines in it, the design and routing of these vital arteries and the prevention of major damages to them are increasingly felt. For example, as the latest, the Sarpol-e-Zahab earthquake ($M_w = 7.3$) on November 12, 2017 in Kermanshah—Iran, broke the main gas pipeline and caused many injuries (www.iiees.ac.ir). In the current situation, given the young age of seismology, it is very difficult to prevent seismic events and predict the exact time of earthquakes (Zinke et al. 2014). However,

✉ Behnam Rahimi
b-rahimi@um.ac.ir

Babak Kheradmand
babak.kheradmand@mail.um.ac.ir

Nasser Hafezi Moghaddas
nhafezi@um.ac.ir

Majid Mehrizi
mmehrizi@yahoo.com

[1] Department of Geology, Ferdowsi University of Mashhad, Mashhad, Iran

[2] Head of Mechanical Engineering at Iranian Gas Engineering and Development Company, Tehran, Iran

with public education, there can be a significant reduction in earthquake damage. Detailed geological and seismo-tectonic examination of each area and the combination of these findings with the results of statistical and probabilistic studies on earthquakes occurring in each area, have the important role in maintaining sustainability as well as continuing the exploit of some things we are going to build.

Although many experiments, studies, tests and mechanical simulations have been carried out on the effect of fault movement on buried pipelines by various scientists (for example: Attari et al. 2016; Youseficoma et al. 2019; Rahimzadeh 2013; Dash and Jain 2007; Mayer and Aydin 2004 and etc.), but most of them have been considered faults as a flat or almost flat surface and most of the mechanical calculus is also the pipes were intended rather than geological impacts. From a structural geological point of view, however, faults are less likely to be flat in nature and often encompass a fault zone of several meters and even kilometer widths, which is virtually impossible to investigate their impact on buried pipelines using conventional mechanical simulation techniques, and the best method in this case is to use advanced and proprietary software.

In this paper, we investigate and simulate the effects of fault movements at intersections with pipeline, using related software, and from this set, to model the impact of fault zone widths on the deformation of gas transmission 20″ pipelines in part of flysch zone in the eastern part of Iran is used in the Iranshahr–Mirjaveh area in Sistan and Baluchestan province (Figs. 1 and 2) and finally its results will be used to optimize the design and routing.

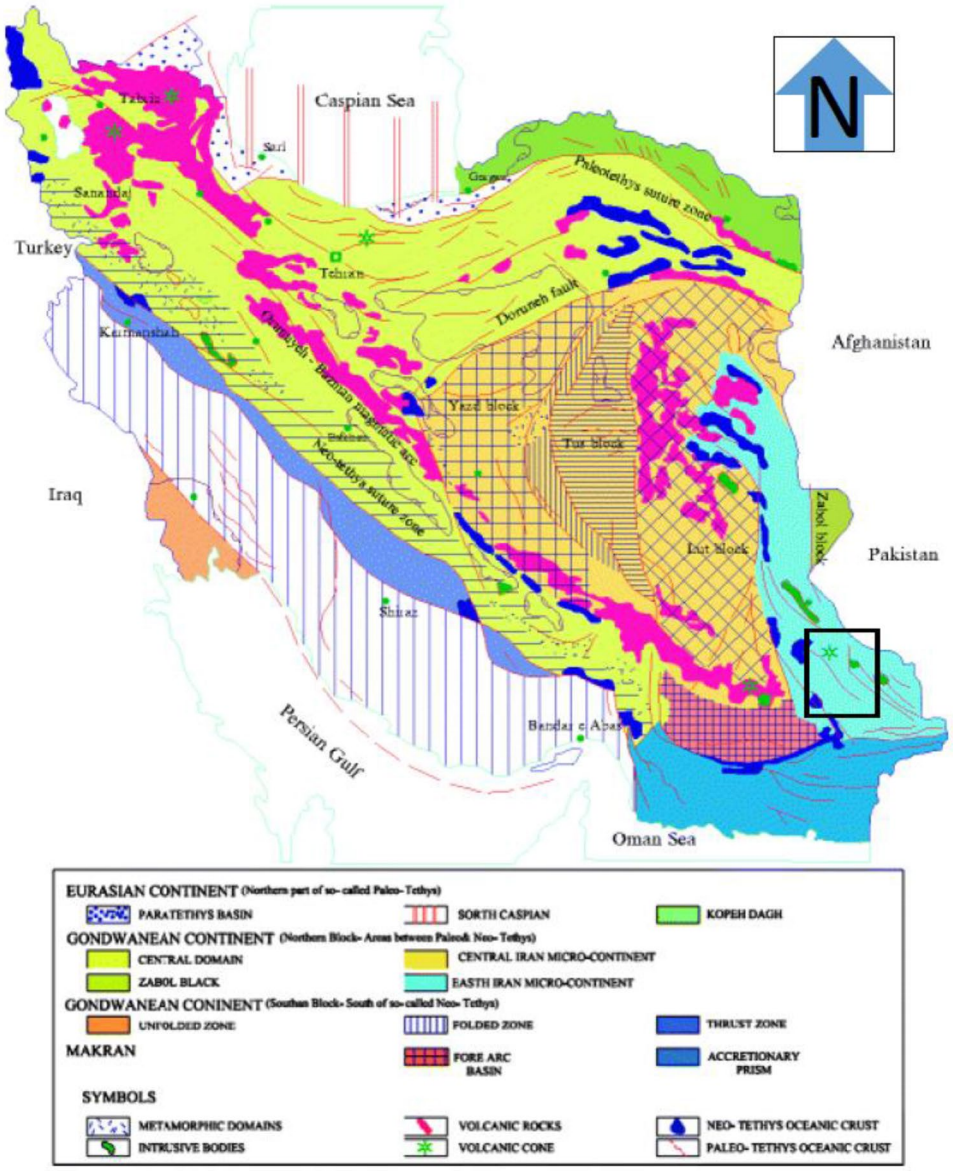

Fig. 1 Important structural-sedimentary zones of Iran (Aghanabati 2004). The study area is represented by a black square in the map

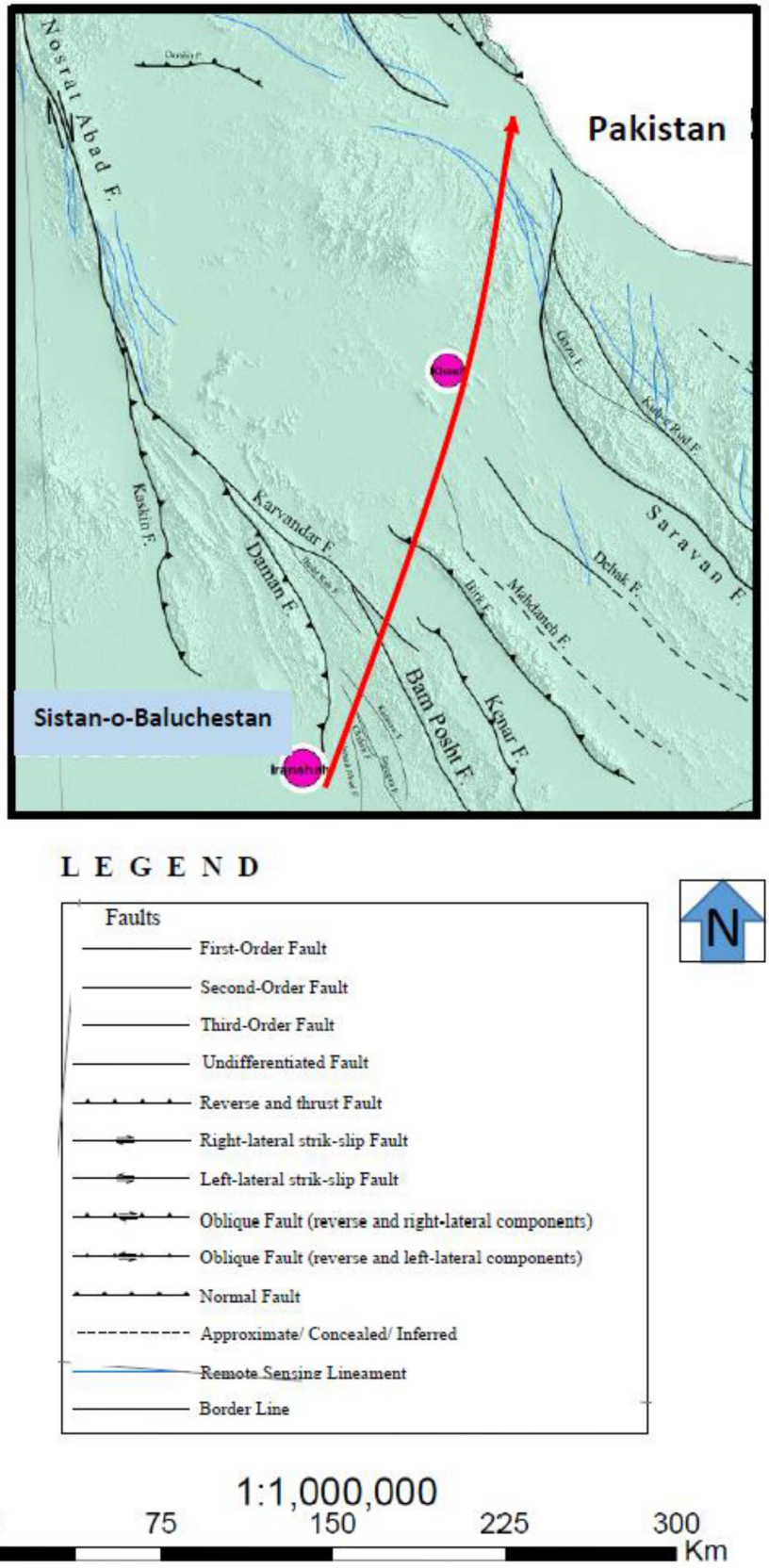

Fig. 2 The direction of study (thick red line) in the Iran fault map on provincial subdivisions (Shaykholeslami et al. 2014)

Tectonic setting

At the beginning of the discussion, we will summarize the tectonic regime in the study area. In general, Iran is located as a trapped plateau between different lithospheric plates and has been affected by a compressional tectonic regime in several respects as a result of the convergence process of the Gondwana and Eurasia parts (Berberian 1981; Aghanabati 2004).

On the west and southwestern sides of Iran, there is an Arab–African plate where the Zagros suture zone is the site of contact of this plate with the Iranian Plateau. It was heading northeast and still continues. It is bounded on the north by the Eurasia Plateau, where the remains are unknown, and is bounded on the east by the Indian Plate, which runs north–northwest. The subduction of the Makran zone to the northeast also causes north–south stresses in this area called the Sistan suture zone (Aghanabati 2004).

The features of the present-day tectonics in this arid, sparsely populated region are broadly understood [e.g., Berberian, 1976, 1981; Berberian and Yeats 1999; Jackson and McKenzie 1984; Nowroozi and Mohajer-Ashjai 1985; Jackson et al. 1995], with major active oblique strike-slip and thrust faults observed in several clearly defined zones. However, little is known of the late Tertiary and younger offsets and slip rates on these active fault systems, results that are important for estimating potential seismic hazard in the region, and also for understanding the regional tectonics.

Right-lateral shear between south-eastern of Iran and Pakistan is accommodated on NW–SE right-lateral strike-slip faults. Little is known of the late Tertiary and younger offsets and slip rates on the active fault systems, results that are important for understanding the regional tectonics. We use observations from satellite imagery to identify displaced geological and geomorphological markers, which we use in conjunction with the overall morphology and orientation of the active fault systems to estimate the total cumulative right-lateral shear. Estimates of cumulative fault movements from offset features and inferred vertical axis rotation of fault-bounded blocks suggest that the late Cenozoic strain is concentrated toward the eastern margin of Iran, along the Sistan shear zone, where bedrock offsets of at least 70 km are observed across the active faults (Walker and Jackson 2004).

As shown in Fig. 2, the faults in the area mainly consist of a major right-lateral strike-slip fault (Nosrat-Abad fault) and its horse tail sprays with a dominant thrust-type mechanism (for example, Daman, Karavandar and Ahmadabad faults), as well as thrust faults independent of the main strike-slip fault (such as the Birk's Mountain thrust). This tectonic regime is due to the movement of the Arabian shield towards the north-northeast as well as the movement of the Indian shield, which now affect the Iranian sub-continent in this part (Walker and Jackson 2004) (Fig. 2). The movement of these plates has been proven by many geological scientists to be highly corroborated by modern advanced survey methods as well as satellite data. In the following discussion, we define the fault parameters in relation to pipelines and then describe the appropriate software for modeling the subject of the article and we will get some interesting results (Tirrul et al. 1983; McCall et al. 1985; Eftekharnezhad et al. 1987; McCall 1997). More of faults have high angle in their outcrop (near to 90°) in this area too.

Research method

In a general sense, the fault refers to fractures in the ground that the rocks on either side of the fracture plate have moved relative to each other. This displacement can range from a few millimeters to hundreds of meters. The energy released during the rapid movement of active faults is the cause of most earthquakes. Of course, in this article, we have inevitably modeled the limited displacement (between 0 and 1.5 m) of fault types.

First, as shown in Fig. 3, for modeling the fault and buried pipe in the fault zone, the parameters are considered as follows: the fault plane angle (Dip angle of the fault) (Ψ) (Fig. 3, b), the angle of entry pipe to fault (angle of pipeline crossing a fault line) (β) (Fig. 3c), the angle between the image of *Y*-axis of the pipeline with the direction of movement vector on the fault plane (θ) (Fig. 3d) (Table 1), and the amount of ground displacement (from 0 to 1.5 m in this research).

Today, many applications have been developed to simulate soil and soil–pipe interactions. The most widely used in industry, research centers and universities are ANSYS Workbench, Plaxis and ABAQUS.

Plaxis 3D Dynamics software, using finite-element method, allows analysis of different structures under static and dynamic loading conditions in a user-friendly environment, due to their different behavioral models for soil. Specific elements have been defined as interface elements to influence the interaction of soil and structures in this software. Interfaces are incremental elements that are added to pages and grids to create an appropriate interaction between structure and soil (Plaxis 3d Reference Manual 2017).

ANSYS finite-element analysis software is used in various fields of engineering analysis. This software provides elements designed to analyze mechanical contact under different conditions. Given the high complexity and variety of these types of elements, special consideration must be given to selecting them for a particular problem. Among these elements is CONTA172, which is defined in three dimensions for page-by-page calling. These contact elements

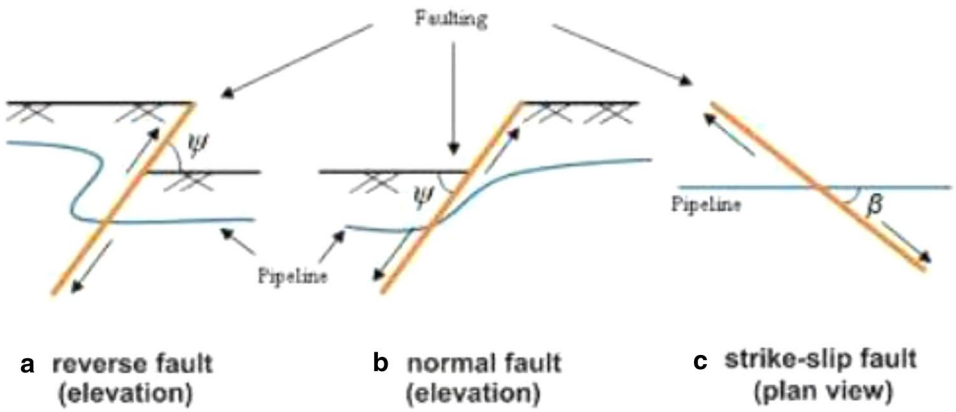

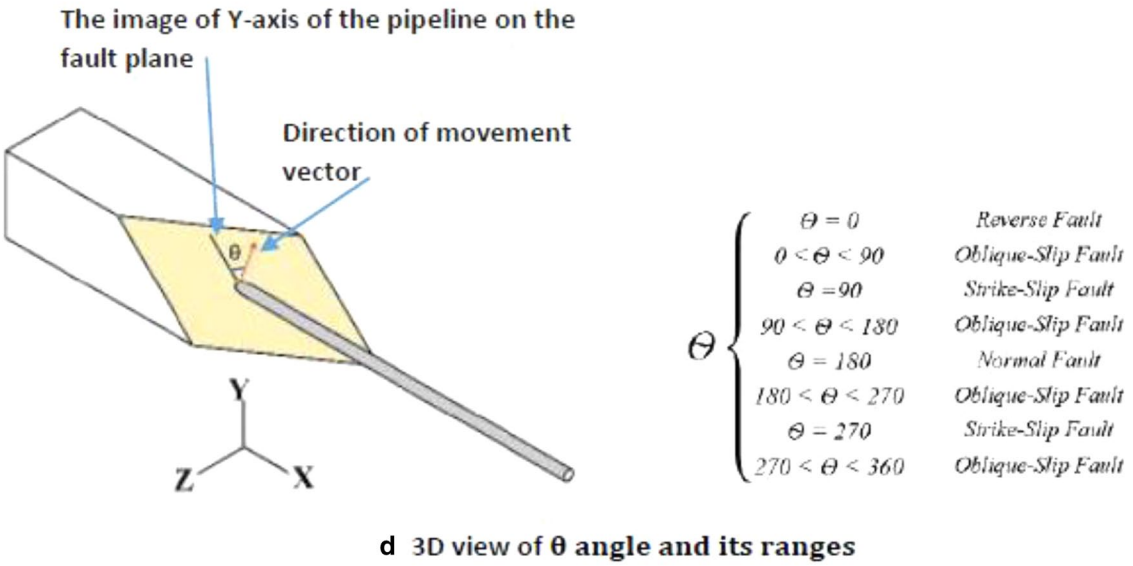

Fig. 3 Different fault types and their effect on pipelines: **a** thrust fault (cross-section) with angle Ψ. **b** Normal fault (cross-section) with angle Ψ. **c** Strike-slip fault (plan view) with angle β. **d** 3D view of angle θ and its ranges on the fault plan (Rofooei et al. 2012; Youseficoma et al. 2019),

Table 1 Types of faults in this analysis

No.	Type of fault	Fault (Ψ) degree plane	The angle of entry tube to fault (β) degree	The angle between the image of *Y*-axis of the pipeline with the direction of movement vector on the fault plane (θ) degree
1	Strike-slip fault	90	90	90
2	Strike-slip–reverse fault	90	90	45
3	Reverse fault	90	90	0

with features such as use for rigid surfaces, high slip allowance and interaction with other elements have removed many limitations for different modes of surface contact and model components (Johnson 2002).

In addition to defining diverse behavioral models for soil, ABAQUS software provides users with two-dimensional (PSI24 and PSI26) and three-dimensional (PSI34 and PSI36) pipe–soil interactions to model the interaction between buried pipe and surrounding soil.

The tube itself can be modeled from the ABAQUS Elements Library with one of the beam, pipe or knee elements. The ground behavior and soil–pipe interaction are also modeled with the relevant elements. These elements have only degrees of freedom in their nodes.

One of the side nodes of these elements is connected to the pipe representative element, and the node at the other end of the interaction element will be connected to a surface that represents the surrounding environment, i.e., the earth. If necessary, the boundary conditions of these nodes can be simulated by moving the Earth (http://femex.ir/abaqus-civil-engineering/). In this research, we have developed GUI software capabilities designed by the Iranian Gas Engineering and Development Company to supervise the research and technology of Iran using a suite of software simulating soil and soil and pipe interactions. Fault intersection modeling with the gas pipeline is used (Youseficoma et al. 2019).

In this method, the inputs required to the software are identified to solve the problem automatically and the various outputs of the problem such as the strain diagram of the pipeline, the displacements and the forces entered on the pipeline are automatically selected in the workspace folder for save software. The completed sample of input data is presented in Fig. 4.

Discussion

Considering the tectonic regime change and sequence from strike-slip to strike-slip–reverse and then reverse from the main fault to fault splays (Kim and Peacock 2004; Mayer and Aydin 2004). In this section, three types of strike-slip, strike-slip–reverse and reverse faults are discussed, respectively, as three common cases in fault terminations in the study area. The common case is addressed in the fault phenomenon. Considering the parameters defined in the previous section, it can be said that for three different angles between the image of *Y*-axis of the pipeline with the direction of movement vector on the fault plane (θ) analysis should be performed. Likewise, the slope parameter and soil type are also needed to investigate the three cases mentioned above. For this simple purpose, the fault plane angles (Ψ) and the tube entry angles (β) are 90° and same for all three types of faults. In this analysis, the criterion for passing the strain limit is in accordance with Table 2. The characteristics and type of soil studied in this section are also presented in Table 3. In this article, due to the limitations in the presentation of images only, the minimum and maximum values are displayed. Obviously, other values fall between these values. In each diagram (Figs. 5, 6 and 7), fault plane is in the middle *X*-axis (0 value) and increases in the positive and negative sides as a fault zone (items a and b, respectively).

The first case: investigation of the effect of pipe damage and breakdown on strike-slip fault ($\theta = 90°$)

In the first case, the strike-slip fault plane angle (Ψ) is assumed to be 90°, the tube entry angle (β) is 90° and the angle between the image of *Y*-axis of the pipeline with the direction of movement vector on the fault plane (θ) is 90° too. In this section, the severity of failure due to fault displacement and the effect of fault width on the extent of failure are studied. Then the problem under study is re-studied by implementing the chosen solution on it.

The effect of increased earthquake intensity on fault displacement has been applied. For this purpose, to investigate the effect of different earthquake intensities on pipeline failure, the amount of strain created was investigated and for different displacements, the strain was calculated and the extent of the resulting failure was monitored.

As shown in the corresponding graphs, the strain rates for different displacements do not.

Change for strike-slip fault ($\theta = 90°$) with increasing fault width (Fig. 5a and b) and as the fault width increases, the strain amplitudes (deformations) will decrease.

The second case: investigation of the effect of pipe damage and breakdown on strike-slip–reverse fault ($\theta = 45°$)

In the second case, the strike-slip–reverse fault plane angle (Ψ) is assumed to be 90° and 90° pipe entry angle (β) and the angle between the image of *Y*-axis of the pipeline with the direction of movement vector on the fault plane (θ) is 45°. In this section, the severity of failure due to fault displacement and the effect of fault dimensions on the extent of failure are studied. Then the problem is re-examined with the proposed optimization strategy.

The effect of increased earthquake intensity on fault displacement has been applied. For this purpose, to determine the effect of different earthquake intensities on pipeline failure, the amount of strain created was investigated and for different displacements, the strain was calculated and the extent of the resulting failure was monitored.

As shown in the diagram, for the strike-slip–reverse fault ($\theta = 45°$) with increasing fault width, the amount of strain created for different displacements is approximately reduced (Fig. 6a, b).

For instance, as shown in Fig. 6a, b, for the zero strike-slip–reverse fault, the extent of the damage with respect to the range that exceeds the standard strain is 10 m or 32.8

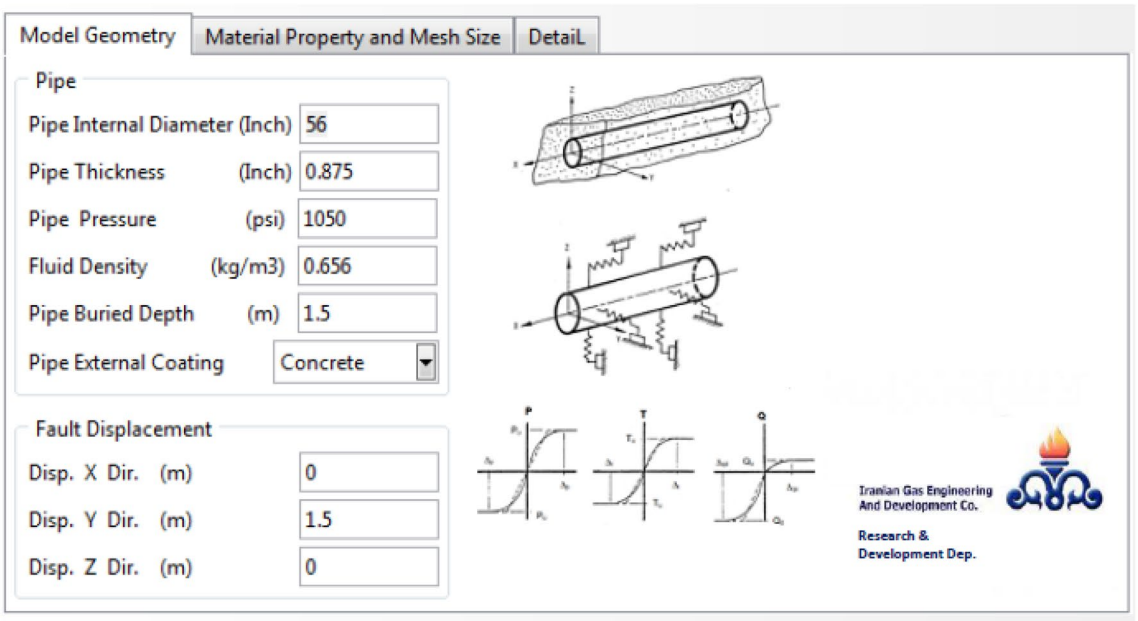

a

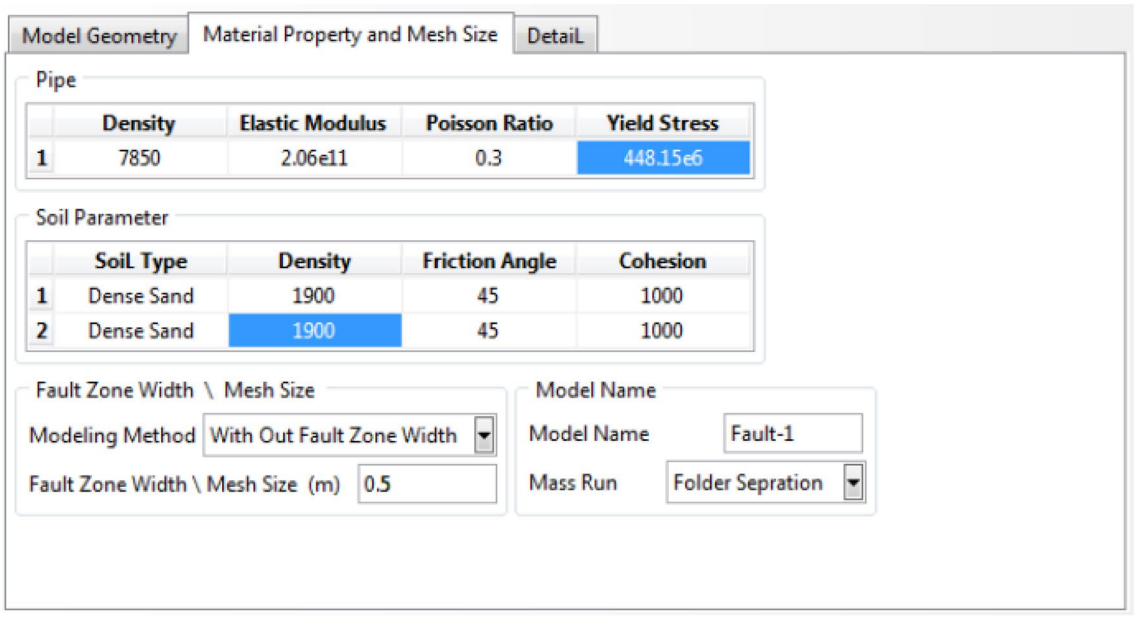

b

Fig. 4 **a**, **b** Tube specifications used in GUI design software (Youseficoma et al. 2019)

Table 2 Strain limit standards (Ghodrati Amiri 2011)

Tube size (In)	Pressure 1050 Psi		Pressure 1400 Psi	
	Critical strain	Thickness	Critical strain	Thickness
20´´	0.0065	0.375	0.0082	0.469
40´´	0.006	0.688	0.0076	0.875
56´´	0.0054	0.875	0.007	1.125

feet, and for maximum fault width of the 5 m is 19 m or 62.33 feet. As the fault width increases, the strain amplitudes (deformations) will decrease.

The third case: investigation of the effect of pipe damage and breakdown on reverse fault ($\theta = 0°$)

In the third case, the reverse fault plane angle (Ψ) is assumed to be 90° angle and 90° tube entry angle (β) and the angle

Table 3 Soil characteristics studied (Sotoodeh Shakib 2019)

Station no.	Km	Handheld no.	Depth (m)	Internal friction angle of soil (Φ Deg.)	Soil sticking coefficient (c_d, kg/cm^2)	Specific soil weight (gr/cm^3)	Poisson's ratio (μ)	Particle density (Gs)
1	0+000	TP1	3.0	25	0.05	1.78	0.38	2.72

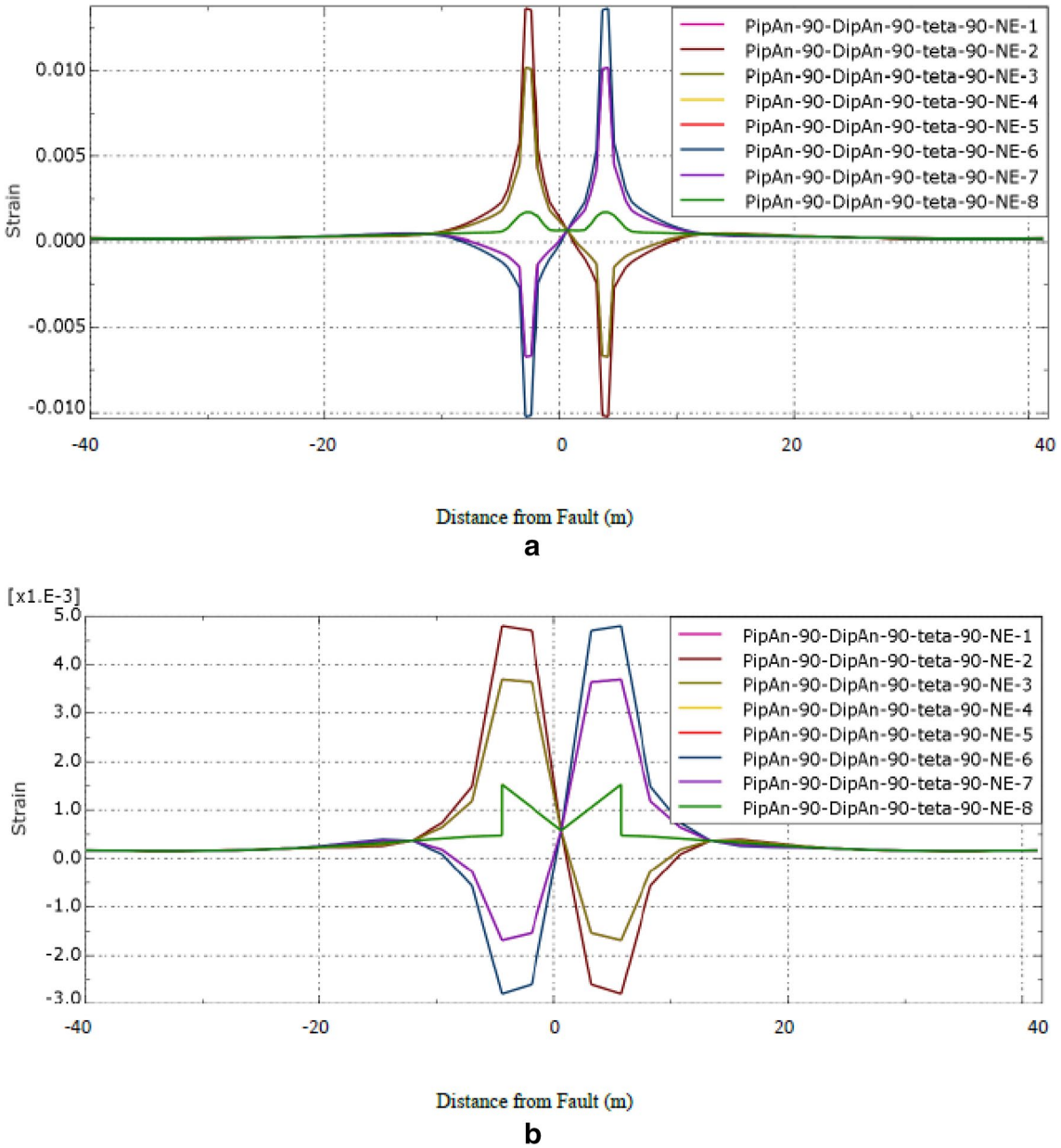

Fig. 5 Tensile and compressive strain graphs of a 20-inch pipe at a depth of 130 cm, a pressure of 1050 lb per square inch for minimum (**a**) and maximum (**b**) strike-slip fault widths. Strain created in strike-slip fault along pipeline for 0 and 5 m fault widths, respectively

between the image of *Y*-axis of the pipeline with the direction of movement vector on the fault plane (θ) is 0°. In this section, the severity of failure due to fault displacement and the effect of fault length on the extent of failure are studied. Then, the problem under study with the optimized method is re-studied.

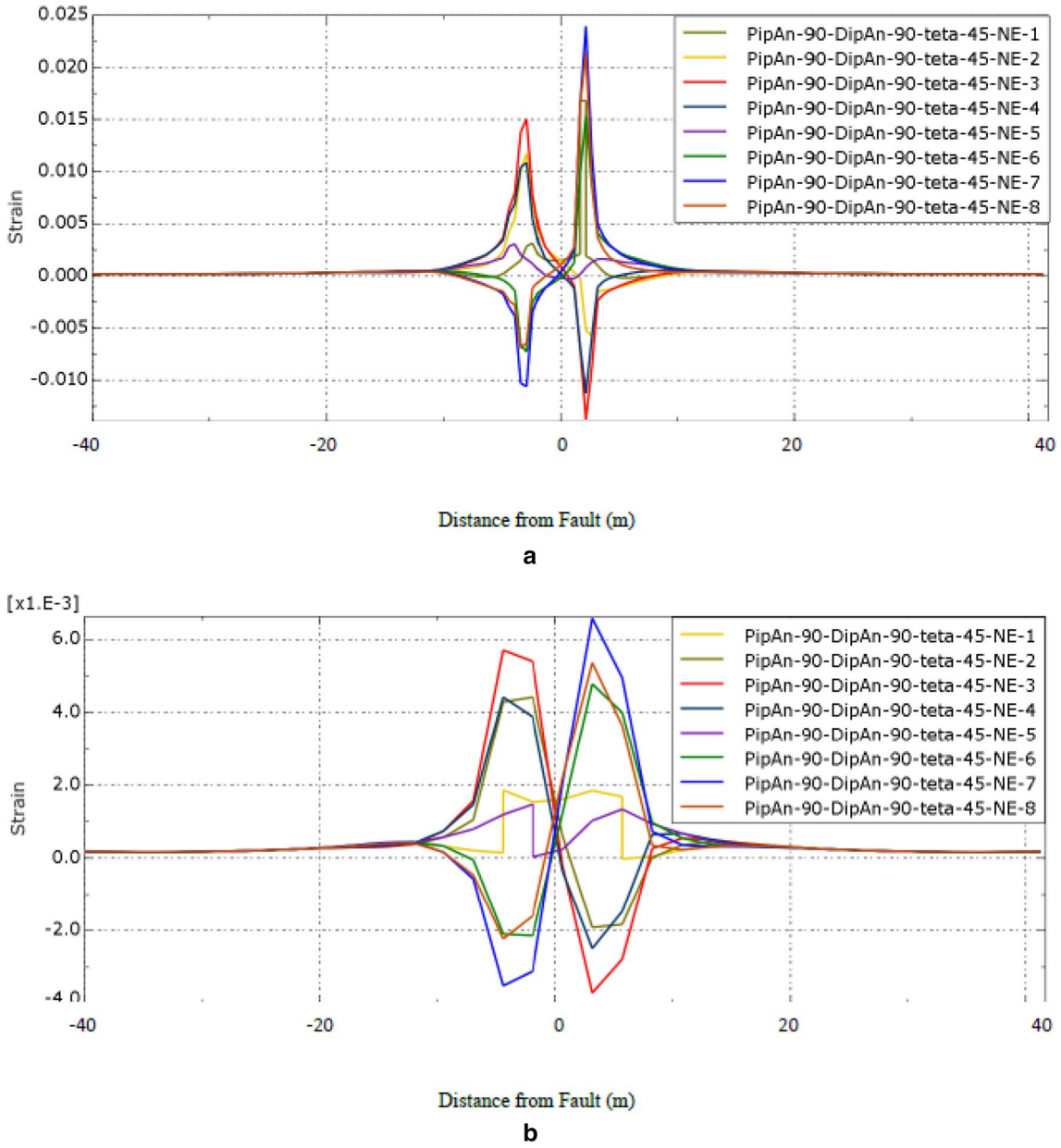

Fig. 6 Tensile and compressive strain graphs of a 20-inch pipe at a depth of 130 cm, a pressure of 1050 lb per square inch for minimum (**a**) and maximum (**b**) strike-slip–reverse fault widths. Strain created in strike-slip–reverse fault along pipeline for 0 and 5 m fault widths, respectively

The effect of increased earthquake intensity on fault displacement has been applied. For this purpose, to determine the effect of different earthquake intensities on pipeline failure, the amount of strain generated is investigated and for different displacements, the pipe strain is calculated and the extent of the resulting failure is monitored.

As shown in the diagram below, for the reverse fault ($\theta = 0°$) with increasing the width of the fault, the amount of strain created for different displacements decreased (Fig. 7a, b). As the fault width increases, the strain amplitudes (deformations) will decrease.

Based on the fault mechanism modeling and their impact on gas pipelines, the following results are obtained:

- Based on the modeling, the increase of fault width of the fault zone from the fault line intersection with the pipeline increases the extent of deformation (bending, torsion, etc.) in the transmission line.
- Based on the simulation and diagrams of reverse faults and strike-slip–reverse faults, at 0–2 m intervals, a very high peak strain is applied, especially from the fault segment on the pipeline due to the focusing. Stress at a finite

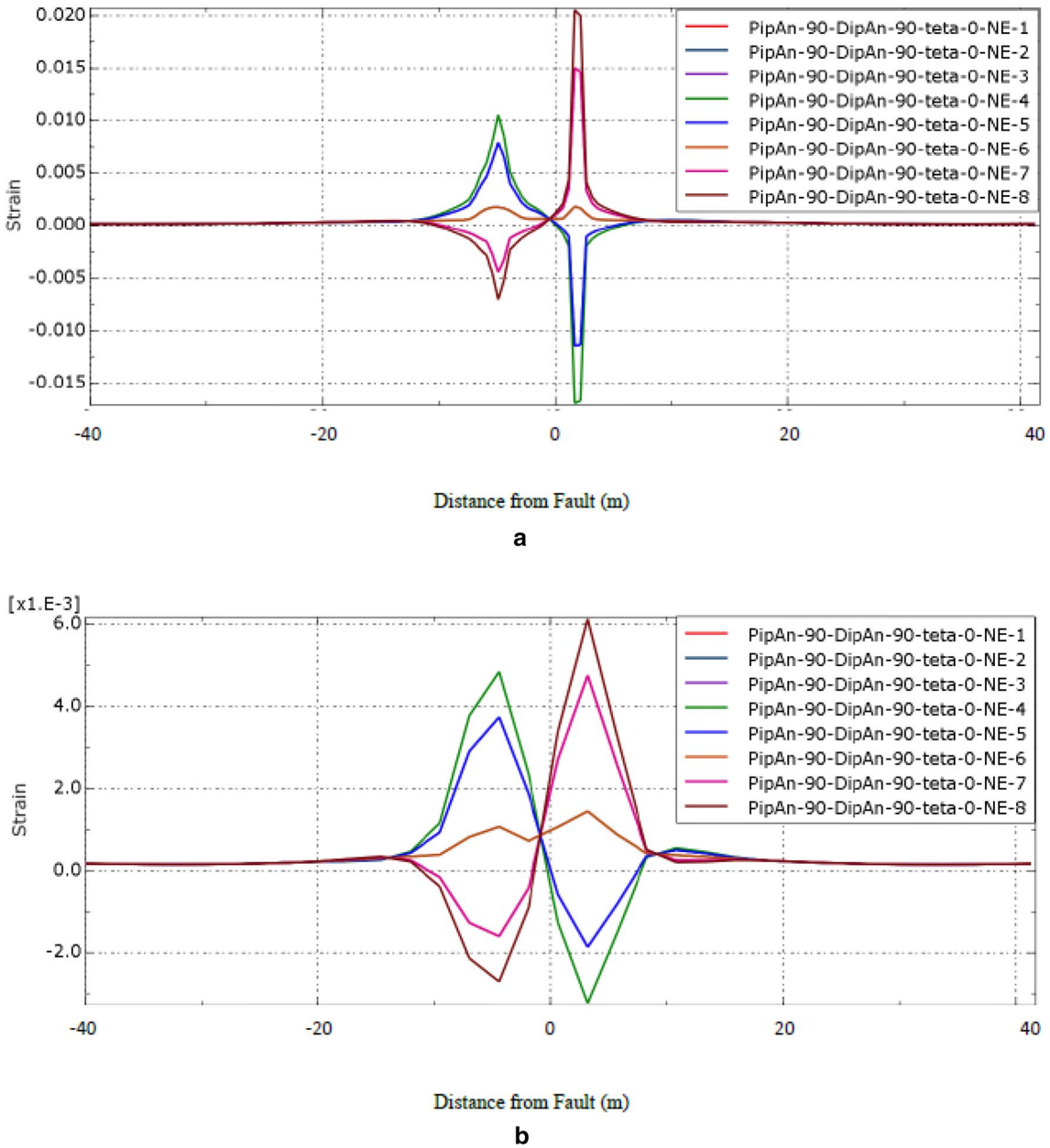

Fig. 7 **a** Tensile and compressive strain graphs of a 20-inch pipe at a depth of 130 cm, a pressure of 1050 lb per square inch for minimum (**a**) and maximum (**b**) reverse fault widths. Strain created in reverse fault along pipeline for 0 and 5 m fault widths, respectively

cross-section is the probability of pipe failure from the side of the slope, but at a distance of 2 m up, the stress concentration is balanced in almost every part of the slope, and the strain concentration is obtained by moving away from the intersection location of the main fault (fault core) and in the fault zone, due to the application and distribution of stress on a wider surface, it decreases (Fig. 8). This is also proved in experimental experiments (Rahimzadeh 2013; Attari et al. 2016).

- Based on the modeling of strike-slip faults, at 0–2 m intervals, a very high peak strain is applied by both plots at approximately equal proportions to the pipeline due to the concentration of stress in a narrow section, the probability of rupture. The pipe is very probable on either side of the wall, but at a distance of 2 m above, the stress concentration is almost equilibrated on both walls, and the strain concentration is obtained by moving away from the intersection location of the main fault (fault core) and due to the fault zone, the stress distribution on a wider surface is reduced.
- In a pipeline design that crosses the fault zone, various parameters such as fault plane angle (Ψ), fault entry

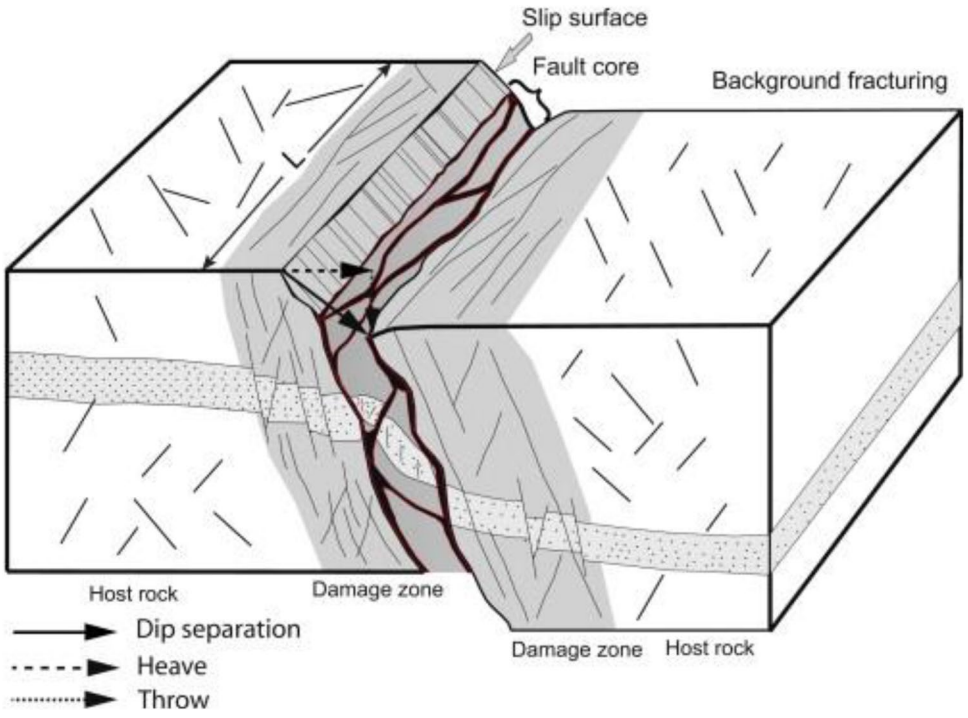

Fig. 8 Schematic diagram describing the fault zone and the extent of the damaged areas

angle (β), and the angle between the image of Y-axis of the pipeline with the direction of movement vector on the fault plane (θ), depth of burial, soil type, and internal pressure of the pipeline are effective. However, only some of the parameters mentioned, such as the angle of entry of the pipe to the fault (β) and the depth of burial of the pipe, can be varied by the design, and the other parameters are unalterable and subject to regional conditions. Therefore, using the parameters mentioned above, the strain created in the pipeline can be minimized to a lesser extent and placed in a better condition.

- For cases where the fault width is not zero, the overall trend of the strain changes in terms of fault width is decreasing. This means that the greater fault width, the same displacement phenomenon results in less strain. For the case where the fault width is zero (which is not practicable of course but is taken into account in theoretical and standard calculations) the problem is contrary to the above procedure and as shown in the Figs. 5, 6 and 7, the maximum strain occurred in this case.

Conclusion

As the result of this study shows, increasing the width of the fault zone increases the extent of failure and at the same time decreases the stress concentration in the main fault, Therefore, the possibility of complete failure of the pipe is reduced by increasing the extent of the fault zone and it is possible to determine the automatic cutoff valves more precisely in accordance with the fault zone privacy and this is very important in the routing of lifelines, especially buried gas pipelines and more precise location of cutoff valves.

Acknowledgements The presenting team would like to thank Mr. Bahram Salavati, the managing director of Iranian Gas Engineering and Development Company, as well as the vice president of engineering and design, Mr. Behnam Mirzaei and head of research and technology, Mr. Ebrahim Esalati for providing the research materials as well as their spiritual support.

References

Aghanabati SA (2004) Geology of Iran, Geological Survey of Iran
ALA (2001) Guidelines for the design of buried steel pipes
Ariman T (1984) Buckling and rupture failures of pipelines due to large ground deformations. College of Engineering and Applied Science, University of Tulsa, Tulsa
Attari NKA, Anvari MD, Hojatjalali H, Momeni M (2016) Seismic response of buried pipelines subjected to normal faulting. Modares Civ Eng J 16:157–169
Berberian M (1976) Contribution to the seismotectonics of Iran (part II), Rep. 39, Geol. Surv. Of Iran, Tehran.
Berberian M (1981) Continental deformation in the Iranian Plateau, Geol. Sur. of Iran, Rep. No. 52
Berberian M, Yeats RS (1999) Patterns of historical earthquake rupture in the Iranian Plateau. Bull Seismol Soc Am 89:120–139
Dash SR, Jain SK (2007) Guidelines for seismic design of buried pipelines. Indian Institute of Technology Kanpur (IITK-GSDMA)
Eftekharnezhad J, Lioyd B, Squire A, Odinga M, McCormic C, Griffiths P (1987) Geological map of Nareh-Now quadrangle-Scale 1:250000, No. M-12, GSI

Ghodrati Amiri GH (2011) Guide to seismic evaluation of oil industry facilities and structures Deputy of Engineering and Supervision of Oil Ministry Projects, Ministry of oil, Iran, Journal No. 41

Jackson J, McKenzie D (1984) Active tectonics of the Alpine-Himalayan belt between western Turkey and Pakistan. Geophys J R Astron Soc 77:185–264

Jackson JA, Haines J, Holt W (1995) the accommodation of Arabia-Eurasia plate convergence in Iran. J Geophys Res 100:15205–15219

Javadi HR et al (2013) Iran fault map on provincial subdivisions. Geological Survey of Iran

Jemioło S, Franus A (2018) User, Abacus 6.14 documentation. vol. IV

Johnson DH (2002) Principles of simulating Contact between parts using ANSYS. Penn State-Erie Univ, Erie, p 12

Kim YS, Peacock DCP (2004) Fault damage zone. J Struct Geol 26:503–517

Mayer R, Aydin A (2004) The evolution of fault formed by shearing across joint zones in sandstone. J Struct Geol 26(5):947–966

McCall GJH (1997) The geotectonic history of the Makran and adjacent areas of southern Iran. J Asian Earth Sci 15(6):517–531

McCall GJH, Eftekharnezhad J, Samiminamin M (1985) Area report, east Iran project (North Makran & South Baluchestan). Geological Survey of Iran, Rep No: 57

Nowroozi AA, Mohajer-Ashjai A (1985) Fault movements and tectonics of eastern Iran: boundaries of the Lut plate. Geophys J R Astron Soc 83:215–237

Plaxis 3d Reference Manual (2017)

Rahimzadeh F (2013) Research project report "Investigation of the destructive effect of faulting phenomena on pipelines and networks nutrition and distribution of gas and its generalization in the Country". Sharif University of Technology

Rofooei F, et al (2012) Full-scale laboratory testing of buried pipelines subjected to permanent ground displacement caused by reverse faulting. In: 15 WCEE, Lisboa

Shaykholeslami M et al (2014) Encyclopedia of Iranian faults. In: Geosciences and mineral exploration organization research institute of earth sciences country. Rahi Publishing

Sotoodeh Shakib A (2019) Project design of the KhooshehKhash gas pipeline base project. Geotechnical & Geological Studies Report, Geocavendish Company, Tehran, Iran

Tirrul R, Griffis RJ, Bell IR, Camp VE (1983) The Sistan suture zone of eastern Iran. Geol Soc Am Bull 94:134–150

Walker R, Jackson J (2004) Active tectonics and late Cenozoic strain distribution in central and eastern Iran. Tectonics 23:TC5010

www.fa.wikipedia.org/wiki/

Youseficoma E et al (2019) Investigation and improvement of gas transmission lines Interference with fault and providing necessary measures design. University of Tehran

Zare M, Kamranzad F (2014) Seismic Dispersion in Iran. J Spatial Anal Environ Hazards 1(4):39–58

Zinke R, Hollingsworth J, Dolan JF (2014) Surface slip and off-fault deformation patterns in the 2013 MW7.7 Baluchistan, Pakistan earthquake: Implications for controls on the distribution of near-surface coseismic slip. AGU-Publications, pp 5034–5050